



College of Agriculture
& Environmental
Sciences

ÉCOLE DE
TECHNOLOGIE
SUPÉRIEURE
Université du Québec

ÉTS
Engineering for Industry

Physics-informed neural networks for modeling water flow and solute transport in unsaturated soils

Presented by: Hamza Kamil^{a,b}

(✉ hamza.kamil@um6p.ma)

Supervised by: Pr. Azzeddine Soulaïmani^a

Pr. Abdelaziz Beljadid^{b,c}

⚙️^a École de technologie supérieure, Montréal, Québec, Canada.

⚙️^b CAES, Mohammed VI Polytechnic University, Ben Guerir, Morocco.

⚙️^c University of Ottawa, Canada.

April 27, 2024

Table of contents

1. Introduction

2. Literature review

3. Methodology

4. Numerical experiment

5. Conclusion



College of Agriculture
& Environmental
Sciences

ÉCOLE DE
TECHNOLOGIE
SUPÉRIEURE
Université du Québec



Introduction

Importance of modeling water and solute transport in soils

Objectives

1. Control water availability to plants and groundwater recharge.
2. Optimize irrigation practices and water resource management.
3. Enhance agricultural productivity and soil fertility.

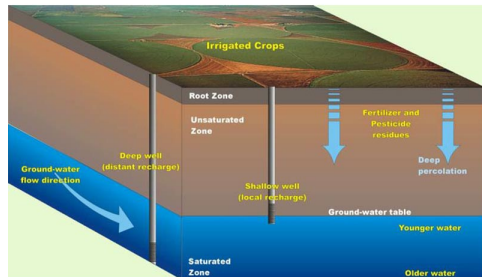


Figure: The coupled processes in the surface-subsurface-groundwater system (Collen, 2019).

The physical model of water-solute transport

The coupled model of water flow and solute transport

$$\left\{ \begin{array}{ll} \frac{\partial \theta}{\partial t} = \nabla \cdot \underbrace{\left[K \nabla (\Psi + z) \right]}_{-q} & \text{water flow} \\ \frac{\partial \theta c}{\partial t} = \nabla \cdot (\theta D \nabla c - c q) & \text{solute transport} \end{array} \right. \quad (1)$$

Table of notations

Notation	Meaning
Ψ	Pressure head, representing the potential energy of water per unit mass due to pressure in the soil.
(t, x)	Time-space coordinates.
K	The unsaturated hydraulic conductivity, indicating the ability of the soil to transmit water.
θ	Soil water content.
q	Water flux.
c	Concentration of solute in the liquid phase.
D	Dispersion tensor, incorporating the effects of molecular diffusion.

Advantages and challenges of using machine learning for water-fertilizers modeling

Advantages

- Accurate predictions of water and solute transport in soils.
- Rapid processing of large datasets.
- Real-time monitoring and rapid decision-making.

Challenges

- Extensive data requirements for training.
- Computational resource demands.
- No incorporation of physical principles and domain knowledge.

Improving water-fertilizer transport modeling with physics-informed neural networks

In this study, we propose using physics-informed neural networks (PINNs) (Raissi et al., 2019), where we integrate physics into the training process of the deep learning model.

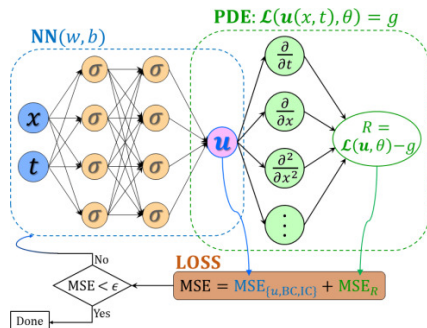


Figure: PINNs.



College of Agriculture
& Environmental
Sciences

ÉCOLE DE
TECHNOLOGIE
SUPÉRIEURE
Université du Québec



Literature review

PINNs for modeling subsurface phenomena

Source	Objective
Bandai and Ghezzehei (2021)	Estimating water surface flux, soil moisture, and related functions using PINNs.
Bandai and Ghezzehei (2022)	Forward and inverse modeling of water flow in unsaturated soils in heterogeneous soils using PINNs.
Depina et al. (2022)	Employing PINNs for identifying unknown soil parameters.
Haruzi and Moreno (2023)	PINNs trained with geoelectrical data for simulating water and solute transport in unsaturated soils with unknown initial conditions.
Faroughi et al. (2023)	Using PINNs with a periodic activation function to accelerate solute transport simulation in heterogeneous soils.



College of Agriculture
& Environmental
Sciences

ÉCOLE DE
TECHNOLOGIE
SUPÉRIEURE
Université du Québec



Methodology

PINNs solvers can be described as Feedforward Neural Networks (FNNs):

$$\begin{cases} y_0 = x \\ y_l = \sigma(W_l y_{l-1} + b_l) \\ \text{for } l = 1, \dots, L \\ \hat{y} = o(y_L) \end{cases} \quad (2)$$

where x represents the input data, L is the number of layers in the neural network, and W_l and b_l are the parameters. σ is the activation function, and o is the output function.

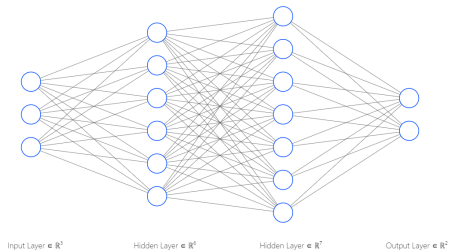


Figure: Diagram of a Feedforward Neural Network (FNN)

Let us consider a specific partial differential equation (PDE):

$$\begin{cases} \frac{\partial u}{\partial t} + \mathcal{N}(u) = 0 & \text{on } [0, T] \times \Omega & \text{PDE} \\ u(0, x) = u_0(x) & \text{on } \Omega & \text{initial condition} \\ u = g & \text{on } [0, T] \times \partial\Omega & \text{boundary condition} \end{cases} \quad (3)$$

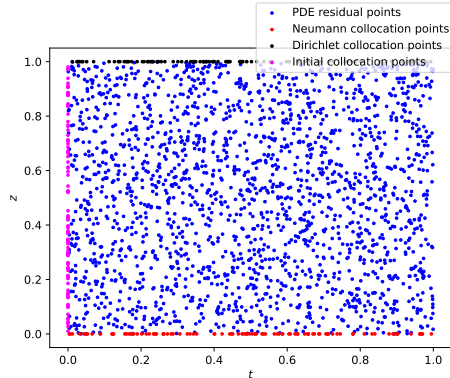
where \mathcal{N} is the spatial operator, Ω is the domain of interest, $\partial\Omega$ is its boundary, T is the final time of simulation, and (u_0, g) are prescribed functions defining initial and boundary conditions.

❗ To address this problem using PINNs, two steps are necessary.

- Step 1: PINNs training

The PINNs inputs consist of time t and space x , segmented as follows:

- $(t_i^r, x_i^r) \in]0, T] \times \Omega$: residual points.
- $(t_i^{ic}, x_i^{ic}) \in \{0\} \times \Omega$: initial collocation points.
- $(t_i^b, x_i^b) \in]0, T] \times \partial\Omega$: boundary collocation points.
- $(t_i^d, x_i^d) \in [0, T] \times \partial\Omega$: available measured data.



- Step 1: PINNs training

For each given data point (t, x) , we compute the following residual functions:

- The residual function \hat{f}_R at (t_i^r, x_i^r) :

$$\hat{f}_R(t_i^r, x_i^r) = \frac{\partial \hat{u}}{\partial t}(t_i^r, x_i^r) + \mathcal{N}(\hat{u})(t_i^r, x_i^r) \quad (4)$$

- The residual function \hat{f}_{ic} at (t_i^{ic}, x_i^r) :

$$\hat{f}_{ic}(t_i^{ic}, x_i^r) = u_0(x_i^{ic}) - \hat{u}(t_i^{ic}, x_i^{ic}) \quad (5)$$

- The boundary residual function \hat{f}_b at (t_i^b, x_i^b) :

$$\hat{f}_b(t_i^b, x_i^b) = g(t_i^b, x_i^b) - \hat{u}(t_i^b, x_i^b) \quad (6)$$

- The data residual function \hat{f}_d at (t_i^d, x_i^d) :

$$\hat{f}_d(t_i^d, x_i^d) = u(t_i^d, x_i^d) - \hat{u}(t_i^d, x_i^d) \quad (7)$$

- Step 1: PINNs training

Now, we can calculate the loss associated with the prediction \hat{u} using the previously defined residual functions:

$$\left\{ \begin{array}{l} J_r(\Theta) = \frac{1}{N_r} \sum_{i=1}^{N_r} \left(\hat{f}_R(t_i^r, x_i^r) \right)^2 \\ J_{ic}(\Theta) = \frac{1}{N_{ic}} \sum_{i=1}^{N_{ic}} \left(\hat{f}_{ic}(t_i^{ic}, x_i^{ic}) \right)^2 \\ J_b(\Theta) = \frac{1}{N_b} \sum_{i=1}^{N_b} \left(\hat{f}_b(t_i^b, x_i^b) \right)^2 \\ J_d(\Theta) = \frac{1}{N_d} \sum_{i=1}^{N_d} \left(\hat{f}_d(t_i^d, x_i^b) \right)^d \end{array} \right. \quad (8)$$

- **Step 1: PINNs training**

Finally, the total loss can be defined as follows:

$$J(\Theta) = \alpha_d J_d(\Theta) + \alpha_r J_r(\Theta) + \alpha_b J_b(\Theta) + \alpha_{ic} J_{ic}(\Theta) \quad (9)$$

where $\Theta = (W, b)$ represents the parameters of the FNN, and $\alpha_d, \alpha_r, \alpha_b, \alpha_{ic}$ are weights assigned to the losses corresponding to measured data, training residual data, boundary conditions, and initial conditions, respectively.

- **Step 2: PINNs final prediction**
After training, the PINN solver is used to predict the solution u of the studied PDE at any given time-space coordinates within our domain.

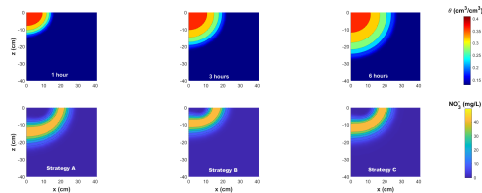


Figure: Final prediction using PINNs.



College of Agriculture
& Environmental
Sciences

ÉCOLE DE
TECHNOLOGIE
SUPÉRIEURE
Université du Québec



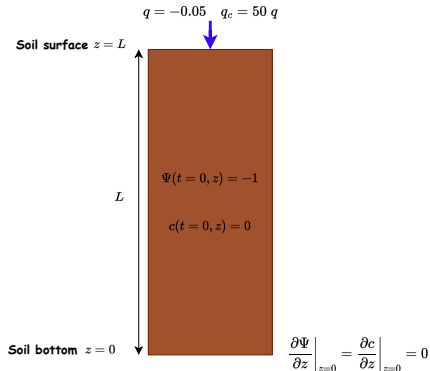
Numerical experiment

Numerical experiment

We consider a 1D loamy soil column with a length L and the following parameters:

$$K_s = 0.2496 \text{ m/day}, \tilde{\alpha} = 3.6 \text{ m}^{-1},$$

$$\theta_s = 0.43, \theta_r = 0.078, n_v = 1.56, L = 1 \text{ m}$$



PINNs settings

PINNs architecture	2 neurons for the input layer. 5 hidden layers with 50 neurons each. 2 neurons for the output layer (1 for Ψ and 1 for c).
Activation function	tanh
Output function	For Ψ neuron: $-\exp$ For c neuron: identity
N_r	10000
$N_b + N_{ic}$	1200
Max iterations	20000
$\alpha_d, \alpha_r, \alpha_b, \alpha_{ic}$	0, 1, 10, 10

PINNs results

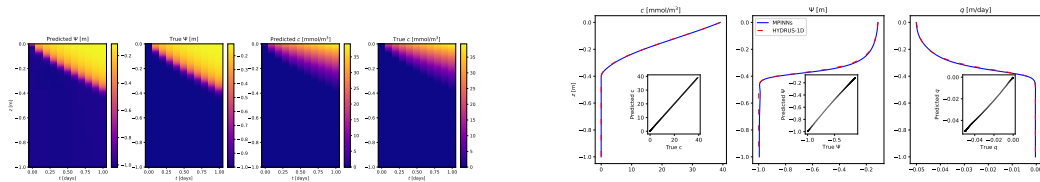


Figure: Comparison of PINN solver predictions for pressure head (Ψ), solute concentration (c), and water flux (q) in the time-space domain $[0, 1] \times [0, 1]$ and at $T = 1$, against true solutions obtained from the HYDRUS-1D software.



College of Agriculture
& Environmental
Sciences

ÉCOLE DE
TECHNOLOGIE
SUPÉRIEURE
Université du Québec



Conclusion

Advantages and challenges of using PINNs for modeling water-fertilizer interactions

Advantages

- Meshless approach suitable for complex geometries without the need to generate a mesh.
- Soft integration of data measurements, particularly effective for inverse problems.

Challenges

- Challenging to train when the solution exhibits steep gradients or when multiple solutes are involved.
- Task-specific; changing any parameter of the PDE requires retraining the model.

References

- Bandai, T., & Ghezzehei, T. A. (2021). Physics-informed neural networks with monotonicity constraints for richardson-richards equation: Estimation of constitutive relationships and soil water flux density from volumetric water content measurements. Water Resources Research, 57(2), e2020WR027642.
- Bandai, T., & Ghezzehei, T. A. (2022). Forward and inverse modeling of water flow in unsaturated soils with discontinuous hydraulic conductivities using physics-informed neural networks with domain decomposition. Hydrology and Earth System Sciences, 26(16), 4469–4495.
- Collen, K. (2019). Nitrate in groundwater data assessment.

Depina, I., Jain, S., Mar Valsson, S., & Gotovac, H. (2022). Application of physics-informed neural networks to inverse problems in unsaturated groundwater flow.

Georisk: Assessment and Management of Risk for Engineered Systems and Geohazards, 16(1), 21–36.

Faroughi, S. A., Soltanmohammadi, R., Datta, P., Mahjour, S. K., & Faroughi, S. (2023). Physics-informed neural networks with periodic activation functions for solute transport in heterogeneous porous media. Mathematics, 12(1), 63.

Haruzi, P., & Moreno, Z. (2023). Modeling water flow and solute transport in unsaturated soils using physics-informed neural networks trained with geoelectrical data. Water Resources Research, 59(6), e2023WR034538.

Raissi, M., Perdikaris, P., & Karniadakis, G. E. (2019). Physics-informed neural networks: A deep learning framework for solving forward and inverse problems involving nonlinear partial differential equations. Journal of Computational physics, 378, 686–707.



College of Agriculture
& Environmental
Sciences

ÉCOLE DE
TECHNOLOGIE
SUPÉRIEURE
Université du Québec

ÉTS
Engineering for Industry

Thank you for your attention

Presented by: Hamza Kamil^{a,b}

(✉ hamza.kamil@um6p.ma)

Supervised by: Pr. Azzeddine Soulaïmani^a

Pr. Abdelaziz Beljadid^{b,c}

✚^a École de technologie supérieure, Montréal, Québec, Canada.

✚^b CAES, Mohammed VI Polytechnic University, Ben Guerir, Morocco.

✚^c University of Ottawa, Canada.

April 27, 2024